OPTICAL SMEAR IN A RESISTIVE GATE SENSOR

T.J. Hazendonk*, A.J. Klinkhamer*

ABSTRACT

To study the effect of optical cross-talk in a resistive gate sensor, a test-circuit has been designed, processed and measured. The cross-talk effect is characterized by the distribution of the collected photo-electrons in the horizontal direction. Some of the results are discussed in relation with the performance of the resistive gate sensor.

INTRODUCTION

The performance of the resistive gate sensor (=RGS) is influenced by the cross-talk of the photo-electrons between the illuminated photo-elements and the opaque vertical transport channels.[1] This optical cross-talk is mainly caused by the spatial spreading of the deeply generated photo-electrons. The resulting "image smear" is in fact similar to that described for other charge transfer image sensors.[2,3]

DESCRIPTION OF THE TEST-CIRCUIT

The physical structure and the principle of operation of the test-circuit is practically identical to that of a 200x300 element RGS.[1] A schematic lay-out of the test circuit has been plotted in fig. 1. After integration, the row-selected signal charge is transferred along the vertical transport channel to a buffer element. During this transfer the gate of the anti-blooming MOST is closed, to prevent charge flow from the channel to the anti-blooming drain. After complete transfer the gate is opened, in order to remove the excess charge of the over-exposed photo-elements. During accumulation of the transferred charge in the buffer element, a previously selected row of signal charge is shifted out by the horizontal CCD-register and detected by the output charge detector. The photo-sensitive matrix contains 80 columns and 160 rows, with an elementary cell dimension of 15 μm (vertically) and 30 μm (horizontally). The selection of the rows is performed externally; row 1, 80 and 160 can be separately selected. Fig. 2 shows the lay-out of two photo-elements with their adjacent transport channels in top view. Cross sections along the lines AA' and BB' are given in fig. 3a resp. fig. 4a.

The test-circuit has been processed in a modified PCCD technology.[4] The vertical and horizontal transport channels have the profiled PCCD structure. These n_1/n-type implanted channels are controlled by either high resistivity or low resistivity poly-silicon gates. The photo-element is a surface MOS capacitor controlled by the poly-silicon row electrode. The p-type substrate is provided with a higher doped p^+ layer to enhance the blue sensitivity. To connect the photo-element with the transport channel the n_1/n-layer of this channel is locally extended and the extension is covered by a thin p^+ type layer ("cross under").

*Philips Research Laboratories
Eindhoven, The Netherlands

SPATIAL DISTRIBUTION OF THE POTENTIAL

In order to analyse the cross-talk effect one has to consider the electron potential in connection with the photo-generation process. For the test-circuit the maximum electron potential Ψ has been calculated, using the abrupt depletion layer approximation. For a given set of technology parameters Ψ has been calculated in one dimension along the cross-sections AA' and BB' of Fig. 2. From the thickness of the depleted layers, the total depth D of the depleted region below the surface can be determined. In fig.s 3b and 3c, the profiles of D and Ψ have been plotted along the line AA', for two resistive gate voltages U_{RG}. In figs. 4b and 4c the profiles of D and Ψ have been plotted along the line BB', for the same values of U_{RG} and two integration gate voltages U_{int}. The voltage U_{RG} applied to the resistive gate electrode varies linearly with the position along the transport channel. In the calculation only those positions have been considered which correspond with $U_{RG} = 0$ V and $U_{RG} = -5$ V. (Theoretically the channel will be inverted below $U_{RG} = -5$ V). The voltage U_{int} applied to the integration gate electrode, is switched between 0-12 V. The integration cycle starts with an empty potential well at $\Psi \simeq 7.5$ V, and reaches its full well condition at the "cross under" potential $\Psi \simeq 1.2$ V. The situation of the small region between the cross-under and the photo-element is not clear, because the calculation does not include the lateral extension of the depleted layers. From the figures it is obvious that

a) for cross-sections AA' a symmetric distribution of D and Ψ is present, while for cross-sections BB' the distributions are asymmetric;
b) the distribution of D and Ψ depends on the position along the transport channel, and the integrated signal charge;
c) the depleted region below the photo-element is at a smaller depth than the regions below the transport channels.

SIMPLE CROSS-TALK MODEL

The photo-sensitive area of the test-circuit is covered with two different layer structures. About 60% of the area is covered with SiO_2/poly-Si/SiO_2, whereas the remaining part is covered only with SiO_2. In the poly-silicon layer, a considerable amount of photons will be absorbed in the spectral region between 0.4-1.0 μm. Another part of the photons is lost by reflection and scattering effects in- and outside the surface layer structure. The photo-electrons generated inside the depleted region below the surface, will be collected in the potential wells according to the distribution of the electric field. The photo-electrons generated outside the depleted layer, diffuse in a random way to the field region before they will be collected. Due to the large depth of the depleted region below the transport channel a noticeable amount of deeply generated photo electrons will be collected by the transport channel. This cross-talk effect will depend on the wavelength of the illumination light, the integrated signal charge and the position along the channel. To simplify the problem, a simple model is used which only takes into account the cross-talk in one dimension at the end of an integration cycle. The cross-talk effect is determined by the different collection efficiencies of the various potential wells. These efficiencies are determined as the integral value at the end of an integration cycle for given position along the transport channel.

Fig. 5 shows schematically a cross-section of some matrix

elements in the horizontal direction. Each window of the light shield corresponds to a photo-element connected to its transport channel by a "cross-under". The symbols a_i and b_i denote the charge collection efficiency of the photo-element resp. the transport channel. The symbols S_i and B_i denote the signals detected by the output charge detector, corresponding to the amount of charge collected by the photo-element resp. the transport channel. The subscript i denotes the position of the elements in reference to the illuminated photo-element. The collection efficiencies a_i and b_i can be calculated from the measured data S_i and B_i, using the relations:

$$a_k = S_k/\Sigma_i(S_i+B_i) \text{ and } b_k = B_k/\Sigma_i(S_i+B_i)$$

METHOD OF MEASUREMENT

For the measurement of S_i and B_i a small vertical slit is projected at one column of photo-elements by means of a high resolution lens. The 15 um slit image illuminates 80 photo-elements at column N = 70, symmetrically around row M = 80, as illustrated in fig. 6a. To read out the signals S_i and B_i, the timing diagram of fig. 7 is used. The signal charge S_i, integrated during a period t_i, is selected at the position N = 70, M = 80. To transfer this signal completely along the transport channel the anti-blooming gate is closed for a period $t_q = t_i/80$. The signal charge of the remaining (79) photo-elements is integrated under the same conditions as the selected one. They are selected shortly after selection of row 80 and removed from the channel by the anti-blooming MOST. After selection of row 80, the transport channels will be read out 15 times, without any row selection. The charge integrated in the transport channels is the background charge B_i, delivered by 80 illuminated photo-elements during a period $t_q = t_i/80$. After 15 cycles background charge B_i, at cycle 16 the signal charge S_o of row 80 is selected and read out together with the background charge B_i of cycle 16. Hence, at cycle 16 the total charge (S_i+B_i) will be read out. To calculate a_i and b_i it is assumed that B_o delivered by 80 photo-elements during a period $t_i/80$, equals B_o delivered by one photo-element during a period t_i. Fig. 6b shows a time series of the output signals, using the timing diagram of fig. 7. (In the figure only the signals S_o, B_o, S_1 and B_1 have been plotted because, for the measured samples, other S_i and B_i signals appear to be zero).

The illumination of the samples is performed with a tungsten light source (T_λ = 2854 K) filtered with 2 mm KG3-IR blocking filter. The spectral band filters have a bandwidth of $\Delta\lambda$ = 9 nm to achieve narrow band illumination. The resistive gate electrode is supplied with a dc-voltage of U_{RG} = -10 V (top-side) and U_{RG} = 0 V (bottom-side). To achieve complete vertical transfer, it has been checked that the time t_q, during which the anti-blooming gate is closed, exceeds the maximum transport time of the electrons. To receive a row of vertically transferred charge, the horizontal CCD register is stopped for a period equal to t_q = 50 usec. The signal charge is read out a four phase CCD register during a period of 200 μsec at a clock frequency f_c = 1 MHz. A charge transfer inefficiency of $\varepsilon < 10^{-4}$ is sufficiently low not to degrade any signal from column positions near the output detector.

RESULTS OF THE MEASUREMENTS

The measurements confirm the expected cross-talk to the transport channels, and its asymmetric character. Within the accuracy of the measuring apparatus only the signals S_o, B_o, S_1 en B_1 could be detected with $S_1 < B_1 < B_o < S_o$.
The dependence of the signal on the calculated collection efficiencies a_o, b_o, a_1 and b_1 is illustrated in fig. 8. In this figure the values of a_i and b_i have been plotted as a function of S_o, reached at the end of an integration cycle, for λ = 545 nm. The maximum amount of signal charge which can be integrated is denoted by S_o^m. In fig. 9 the wavelength dependence of the collection efficiencies is demonstrated. In this figure the a_i and b_i have been plotted as a function of λ, for a signal charge $S_o = 2/3\ S_o^m$ reached at the end of an integration cycle. The signal dependence and wavelength dependence is evident for the a_o, b_o and b_1 components, the behaviour of the a_1 component is less clear. Because even at λ = 445 nm a small response of the a_1 component is measured, it is believed that a small part of the cross talk originates from scattering effects in the surface layers (light piping).

The measured samples are chosen from one batch and are selected for uniformity in photo response and transport properties. The measured S_i and B_i values are not constant from day to day. In particular the S_1 and B_1 values show large deviations from their average values. The origin of these fluctuations is not clear; they appear to correlate with small variations of the temperature and the integration voltage. However, these fluctuations have been found to be smaller than the fluctuations found in S_i and B_i when measured for different columns of one sample.
The a_i and b_i data of figs. 8 and 9 result from S_i and B_i values averaged over 10 columns of the measured samples. The accuracy of the a_i and b_i data is expressed in their rms-value σ.
For the data plotted in figs. 8 and 9, it has been found that:
σa_o = 10%, σb_o = 7%, σa_1 = 65% and σb_1 = 17%.
In figs. 10 and 11 compositions of the collection efficiencies a_o, b_o and b_1 have been plotted as a function of S_o and λ, to illustrate the signal dependence and the wavelength dependence. The data have been calculated from measurements of one selected sample at N = 70.
Figs. 8-11 show that at medium levels of signal charge the a_1 and b_1 components are small in comparison with the a_o and b_o components. In that case it is justified to use the approximation: $b_o \simeq 1-a_o$.

DISCUSSION

The cross-talk between the photo-element and the transport channels has a noticeable effect on the performance of an RGS. For an arbitrary image, the signal charge S_o varies with the position along the vertical transport channel. The total background charge is determined by all contributions of the illuminated photo-elements along the transport channel. To simplify the problem of the signal dependent background charge, it is assumed that the irradiance of the illumination light together with a_o and b_o is independent of the position along the channel.
Consider now a sensor containing N integration rows of which M^* rows are uniformly illuminated by incident light of irradiance H. During an integration cycle t_i, for narrow spectral band

illumination at low light levels, the photo-element will integrate a signal charge

$$S_o = K\, a_o H t_i \qquad (1)$$

where K is a function of the wavelength and spectral bandwidth of the illumination light, the absorption efficiency, the quantum efficiency, the geometry and the integration voltage of the photo element, and the charge transfer function of the output detector. However, for narrow spectral bandwidth illumination and stationary device operation, K is assumed to be constant.

The maximum amount of signal charge which can be integrated by the photo element is

$$S_o^m = K\, a_o H^m t_i \qquad (2)$$

where H^m denotes the saturation level of exposure. During the period t_q that the anti-blooming gate is closed the M^* illuminated photo-elements deliver a background charge

$$B_o = K\, b_o H M^* t_q \qquad (3)$$

This background charge will be added to the selected signal charge, so that a total signal $(S_o + B_o)$ will be read out. To characterize this so called "image smear", a ratio S_o/B_o is defined.
Hence, below the saturation level of exposure $(H < H^m)$ it is found that

$$S_o/B_o = a_o/b_o pq \qquad (4)$$

where $p = M^*/M$, the column illumination fraction and $q = t_q/t_l$, the fraction of the line read out time that the anti-blooming gate is closed.

To handle over-exposure, the integration voltage of the photo-element is enlarged during a certain period of the line read out time.[1]
After return to its normal operation level, the excess charge in the photo-element spills to the transport channel. Due to this mode of operation, in the situation of over-exposure the maximum amount of signal charge S_o^m, will be read out. However, the M^* over-exposed photo-elements still deliver a background charge B_o proportional to the irradiance H. Hence beyond the saturation level of exposure $(H > H^m)$ it is found that

$$S_o/B_o = S_o^m/B_o = a_o/b_o\, pqr \qquad (5)$$

where $r = H/H^m$ the over-exposure factor.
Eqs. 1 and 2 suggest a linear response between the irradiance H and the signals S_o resp. B_o. However, due to the signal dependence of a_o and b_o a non-linear relation is present. From the measurements of $(S_o + B_o)$ versus H and B_o versus H, the non-linearity between S_o and H can be determined. Due to the signal dependence of b_o each column delivers its own amount of background charge to the selected signal charge.
As a result of the vertical image smear in all columns

the spatial resolution in the horizontal direction will be decreased. Suppose that the condition $S_o^m \geq 100\ B_o$ represent in an acceptable resolution loss. Suppose that a real image can be approximated by a uniform illumination of the whole column to half the saturation level then it holds that $p = 1$, $S_o = \frac{1}{2} S_o^m$. For the worst case value of $q = 0.5$, it is found from eq. 4 that a_o/b_o has to be larger than 25 to fulfil the condition. In the case of over-exposure it is assumed that 10% of the column will be submitted to uniform illumination beyond the saturation level. With $p = 0.1$, $q = 0.5$ and $S_o = S_o^m$, it is found from eq. 5 that : $r \leq a_o/5b_o$, to fulfil the condition of $S_o^m \geq 100\ B_o$. With the minimum value $a_o/b_o = 25$ found for the sitation below saturation exposure, the over exposure factor r is limited to the value $r \leq 5$.
This value is far below the theoretical value $r = M/U$ which can be achieved in a RGS without image smear. In this relation U denotes the fraction of the line read out time that the integration voltage is enlarged. For the test-circuit at medium levels of signal charge, it is found that the ratio a_o/b_o is 1-2. This ratio is certainly too low to achieve an acceptable video TV image.
In an improved design of the 200x300 element RGS, the configuration of the photo-element has been altered. The surface channel MOS capacitor is replaced by a buried channel capacitor, to extend the depleted region below the photo-element.
With the improved RGS design a good video image has been obtained.
This better result is confirmed by preliminary measurements of the collection efficiencies, which shows that the ratio $(a_o/b_o) > 10$.

CONCLUSIONS

To study the effect of optical cross-talk in a resistive gate sensor, a test-circuit has been designed, processed and measured. The measurements of the collection efficiency confirm the prediction of an appreciable cross-talk between the photo-element and the adjacent transport channels. This cross-talk results in a non-linear photoresponse, vertical image smear, horizontal resolution loss and putssevere limits to the anti-blooming capacity.

Better results have been obtained with an improved design of the 200x300 element RGS.

ACKNOWLEDGEMENT: The authors wish to thank T. Smit for his technical assistance and H. Peek for processing the circuit.

Eindhoven, July 1979

REFERENCES

1. H. Heyns, J.G. van Santen
IEEE Trans. Electron. Dev., vol. ED-25, pp. 135-139, 1978

2. R.H. Dyck, W. Steffe,
Proc. 1978 CCD Application Conf., pp. 1-55/1-66

3. S.B. Campana,
Optical Engineering, vol. 16, pp. 267-274, 1977

4. H. Peek,
IEEE. J. on Solid-State Circ., SC-11(1976), p. 167

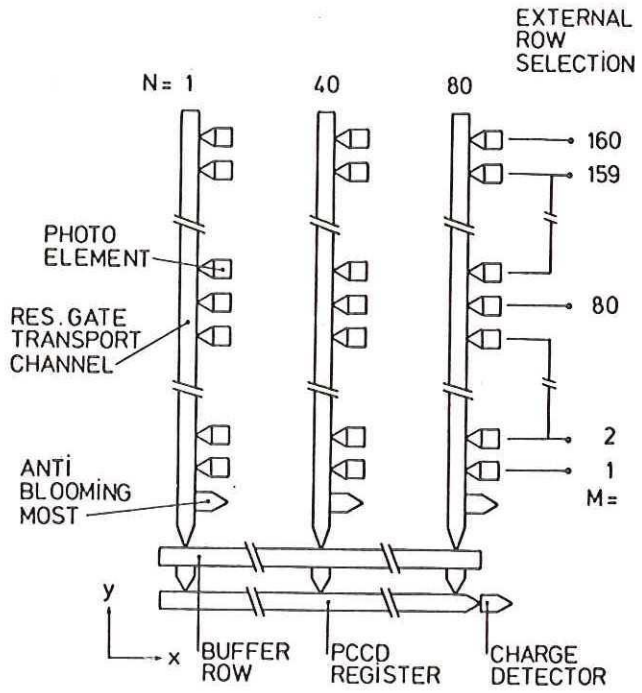

Fig. 1 Schematic lay-out of test-circuit.

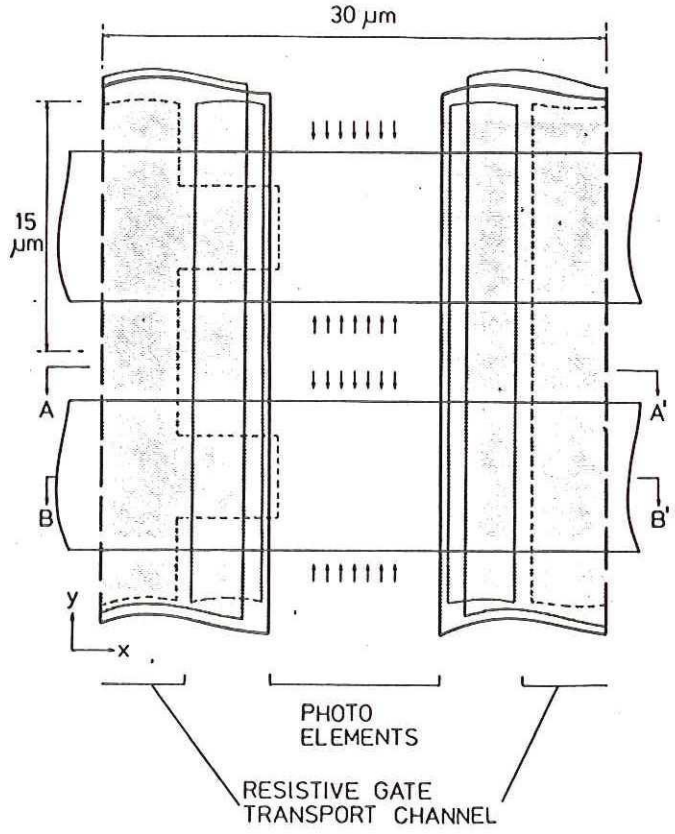

Fig. 2 Lay-out of two photo-elements with adjacent transport channels.

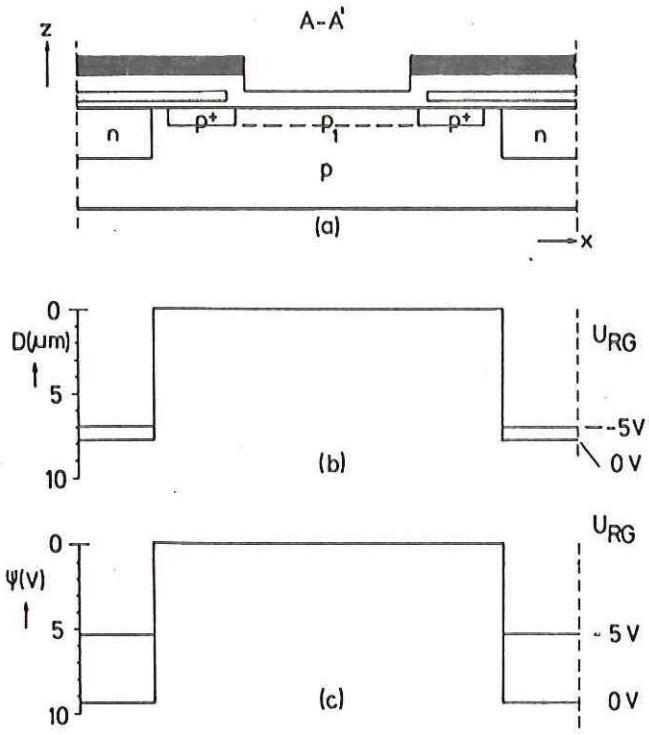

Fig. 3 Depth of depleted layer (b) and electronpotential (c) for cross-section (a).

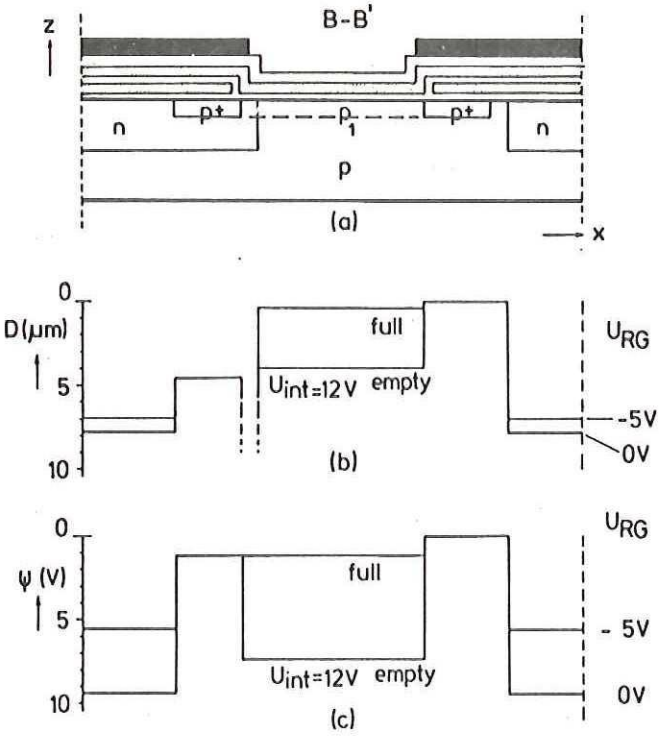

Fig. 4 Depth of depleted layer (b) and electronpotential (c) for cross-section (a).

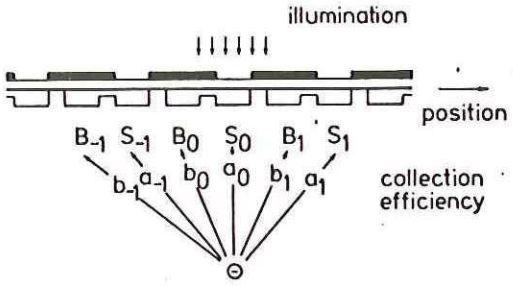

Fig. 5

Illustration of simplified cross-talk model

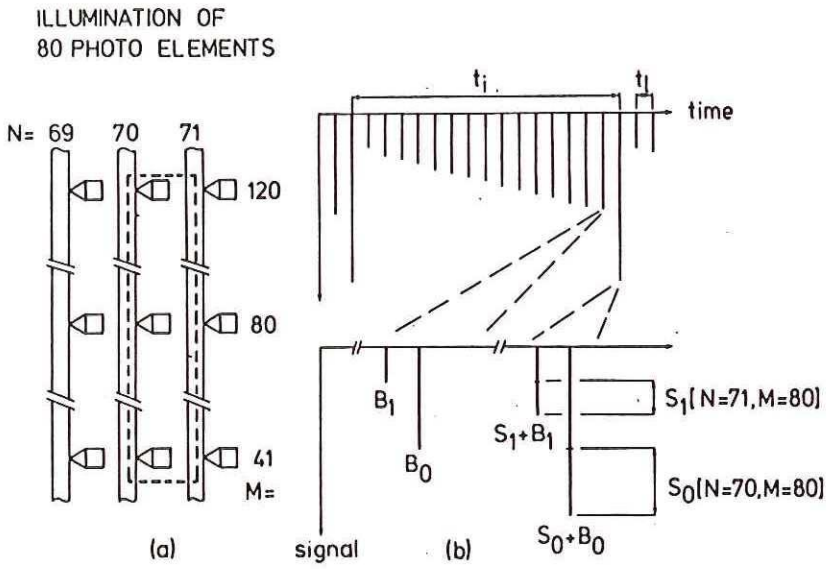

Fig. 6 Illustration of illumination input (a) and measured signal output (b).

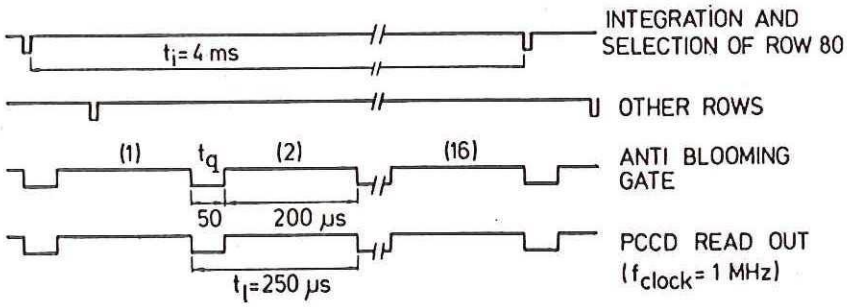

Fig. 7 Timing diagram for cross-talk measurements.

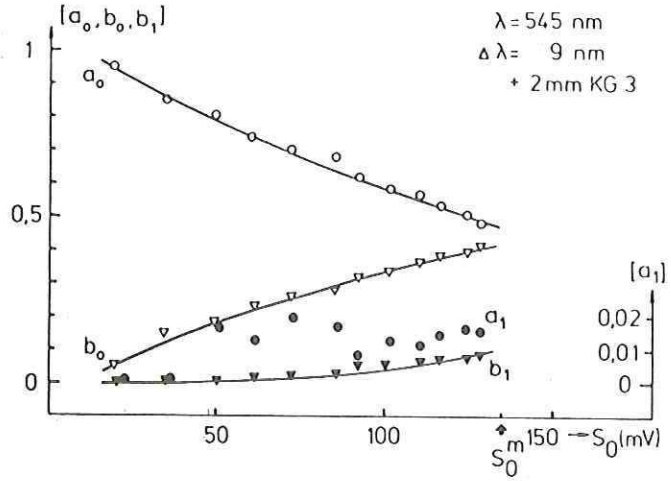

Fig. 8

Plot of collection efficiencies versus signal level at the end of an integration cycle, for a fixed wavelength.

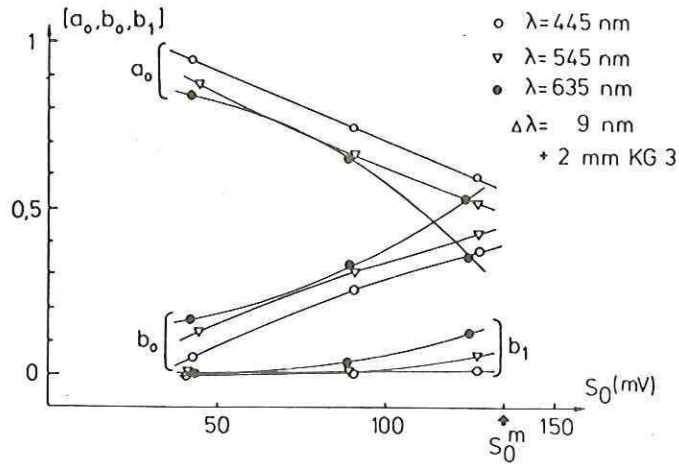

Fig. 9

Plot of collection efficiencies versus wavelength, for a fixed signal level at the end of an integration cycle.

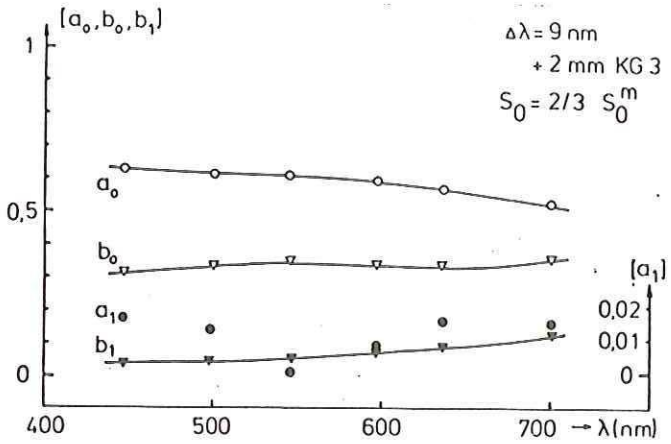

Fig. 10

Plot of the signal dependence of some collection efficiencies.

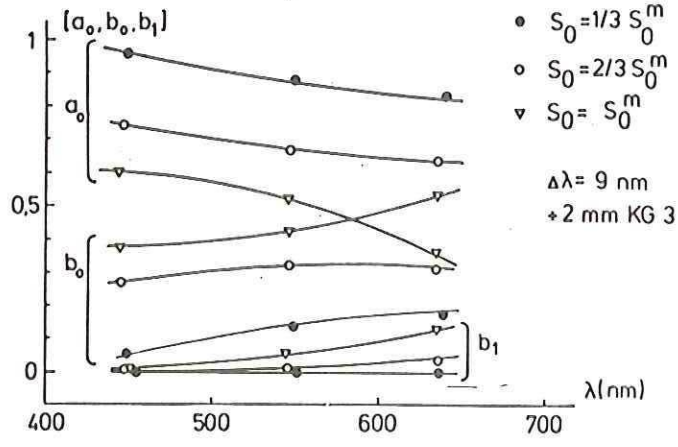

Fig. 11

Plot of the wavelength dependence of some collection efficiencies.